Photophoretic Light-flyers with Germanium Coatings as Selective Absorbers

Zhipeng Lu[1], Gulzhan Aldan[2], Danielle Levin[1], Matthew F. Campbell[2], and Igor Bargatin[2,3]

Abstract: The goal of ultrathin lightweight photophoretic flyers, or light-flyers for short, is to levitate continuously in Earth's upper atmosphere using only sunlight for propulsive power. We previously reported light-flyers that levitated by utilizing differences in thermal accommodation coefficient (TAC) between the top and bottom of a thin film, made possible by coating their lower surfaces with carbon nanotubes (CNTs). Such designs, though successful, had relatively high thermal emissivity (>0.5), which prevented them from achieving high temperatures and resulted in their transferring relatively low amounts of momentum to the surrounding gas. To address this issue, we have developed light-flyers with ultrathin undoped germanium layers that selectively absorb nearly 80% of visible light but are mostly transparent in the thermal infrared, with an average thermal emissivity of <0.1. Our experiments show that germanium-coated light-flyers could levitate at up to 43% lower light irradiances than mylar-CNT disks with identical sizes. In addition, we simulated our experiments using a semiempirical model, allowing us to predict that our 2-cm-diameter disk-shaped germanium-coated light-flyers can levitate in the mesosphere (altitudes 67-75 km) under the natural sunlight (1.36 kW/m^2). Similar ultrathin selective-absorber coatings can also be applied to three-dimensional light-flyers shaped like solar balloons, allowing them to carry significant payloads and thereby revolutionize long-term atmospheric exploration of Earth or Mars.

Unmanned aerial vehicles (UAVs) can potentially carry out extensive, long-lasting, and cost-effective exploration of Earth's atmosphere. One proposed kind of small UAVs—sunlight-powered photophoretic flyers, or light-flyers—can levitate in mid-air using a temperature gradient across a nano-cardboard plate [1][2] or by taking advantage of a difference in the thermal accommodation coefficient (TAC) between two sides of a thin film [3].

Previously reported light-flyers were not yet suitable for deployment in Earth's upper atmosphere or on Mars because they required irradiance levels many that of natural sunlight. The natural sunlight irradiance is 1.36 kW/m^2 under normal incidence in the mesosphere or stratosphere, approximately 1 kW/m^2 at sea level on Earth, and <0.6 kW/m^2 on Mars. In contrast, we previously reported levitation of 6-mm-diameter mylar-CNT disks at irradiances above 5 kW/m^2 [3] and 8-mm-wide nano-cardboard plates at irradiances above 10 kW/m^2 [1], with both done at room temperature in a vacuum chamber.

Recent theoretical studies suggest the possibility of not just levitation, but also of carrying significant payloads, in Earth's upper atmosphere, where the ambient temperatures are much lower than at sea level. For instance, Schafer et al. [2] predicted that a 10-cm-diameter disk using alumina-based nano-cardboard composites could carry a 0.3-gram payload in the stratosphere, roughly 10 times the craft's mass and sufficient for simple silicon-based sensors. Additionally,

[1] Department of Chemistry, University of Pennsylvania, Philadelphia, PA.
[2] Department of Mechanical Engineering and Applied Mechanics, University of Pennsylvania, Philadelphia, PA.
[3] Corresponding author. Email: bargatin@gmail.com.

Celenza et al. [4] simulated three-dimensional meter-scale porous structures capable of carrying much larger kilogram-scale payloads in the upper mesosphere (see Fig. 1(b)). Though holding significant promise, these results have yet to be practically demonstrated. Laboratory experiments are therefore crucial to confirm the lift forces generated by thermal transpiration or Knudsen pump mechanisms and to move toward real-world applications of these light-flyers.

All other things being equal, the photophoretic force increases with decreasing thermal emissivity, because this typically causes the light-flyer to be hotter relative to the ambient atmosphere. Similarly increasing TAC difference between the two surfaces is also beneficial because this results in a greater momentum differential between gas molecules colliding with the top and bottom surfaces [3]. Since all TAC values in air are fairly close to unity due to a molecularly thin organic layer spontaneously formed under ambient conditions [5], it is difficult to increase the difference in TAC beyond 10-20% even for clean well-characterized surfaces [6][7]. However, it is possible to create light-flyers with very low thermal emissivity values by coating them with a selective absorber that has a high absorptivity for the solar spectrum but low emissivity in the thermal infrared (5-15 μm wavelength). Many semiconductors possess such optical properties as long as their bandgaps fall at energies between those of the visible and thermal infrared spectra (i.e., 0.35-1.4 eV [8]). Among these options, undoped germanium is easy to deposit, nearly transparent in the thermal infrared spectrum [9] and thus has very low emissivity, making it an ideal candidate for our selective absorber.

As detailed below, our use of germanium resulted in a significant reduction in the light irradiance needed for levitation from 2.5 kW/m^2 CNT-coated light-flyers to just 1.5 kW/m^2 for germanium-coated flyers. To corroborate our findings, we also measured the optical and surface properties of germanium and developed a theoretical model to predict the light-flyer's levitating performance in both the laboratory and in Earth's mesosphere. Importantly, our model predicts that natural sunlight (~1 kW/m^2) would be sufficient for levitation in the mesosphere because the ambient temperature there are much lower than in our laboratory experiments.

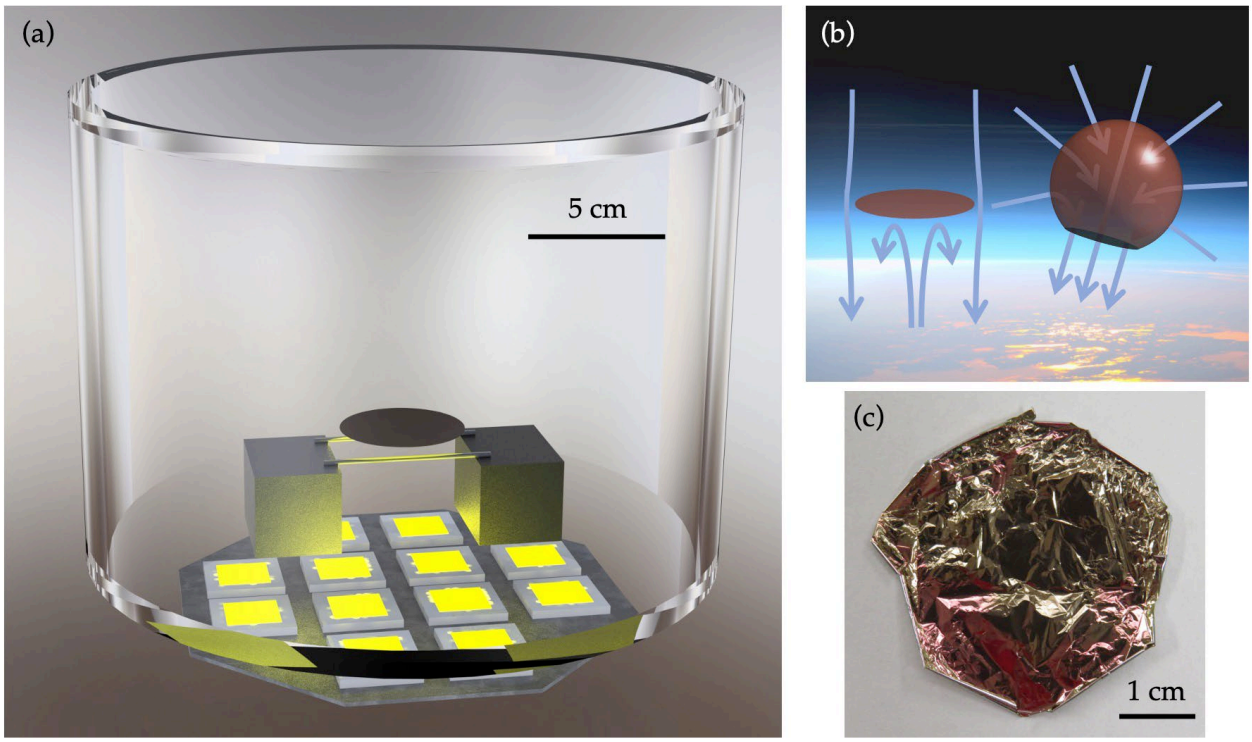

FIG. 1. (a) Schematic diagram of the experimental setup consisting of an acrylic vacuum chamber, a 4-cm-diameter germanium-coated light-flyer, two 2.4-mm-diameter aluminum rods on two 4.5-cm-tall substrates, and 12 LEDs below the chamber. (b) Conceptual diagram of a germanium-coated light-flyer disk (left) and solar-photophoretic balloon (right) in the mesosphere. The background is courtesy of NASA [10]. (c) Photograph of a 4-cm-diameter alumina-germanium-mylar-germanium light-flyer. We observed that the spontaneous wrinkling of this light-flyer helped to maintain its flat shape during levitation.

We fabricated disk-shaped light-flyers by sputtering germanium as the light-absorbing layer on both sides of a 500-nm-thick mylar film, followed by atomic-layer-depositing (ALD) a 50-nm-thick layer of alumina onto one side of the film to enhance its light-flyer's mechanical and thermal robustness (see *Supplemental Material* [11] for detail). Depositing alumina on both sides creates a symmetric structure resulting in no significant TAC difference between the top and bottom sides. Hence, for the purpose of this study, only one side of the film has the alumina. In the final stage of the fabrication process, we laser-cut circular disks of different sizes from our germanium-mylar-germanium-alumina films. Fig. 1(c) shows a representative germanium-coated disk, where the spontaneous wrinkling of the surfaces resulted from the instinct non-uniform stresses in the mylar film. This feature increased the thermal resilience since, in our experience, wrinkled samples bent and curved less than planar samples under intense light.

We tested our light-flyers in a cylindrical acrylic vacuum chamber and illuminated them from below using an arrangement of twelve 100-W LED arrays, which created irradiance of up to 6 kW/m^2 (6 Suns). In a single experiment, we held the chamber pressure constant while gradually increasing the light irradiance until the light-flyer lifted off; we then repeated this procedure at different pressures. Notice that the LED light generally came from below the light-flyer, in contrast to the real-world deployment in the mesosphere where sunlight shines from above. However, we

have previously determined that the photophoretic force is independent of the direction of the incoming light, since the top side of the light-flyer is transparent and the light is always absorbed in the germanium layer on the bottom side.

Vacuum chamber levitation experiments can be impacted by the ground effect, in which an enhanced lift force is generated when the light-flyer is close to the chamber floor [12]. To avoid overestimating the lift force due to this effect, we followed the guidelines from Ref. [12] for minimizing the launchpad-associated ground effect. This involved using a sparse launchpad consisting of two 2.4-mm-diameter aluminum rods, as shown in Fig. 1 (a). These thin aluminum rods exhibited a minimal ground effect similar to that of J-shaped steel wires from Ref. [11], as shown in Fig. S2. We used the rods rather than the wires because they were more convenient in sample loading and testing. We also positioned the launchpad about 4.5 cm above the chamber floor, a distance greater than the diameter of the largest sample, in order to minimize the floor-associated ground effect [11].

Figure 2 illustrates the impact of the selective-absorption coating by comparing the levitation of germanium-coated light-flyers to those with previously reported CNT-coatings [3][12]. It can be seen that, for all disk sizes, the irradiance required for levitation is lower for Ge-coated light-flyers, demonstrating the impact of this type of coating. Specifically, the minimum irradiances needed for levitation were 29%, 39%, and 43% lower for 2, 3, and 4-cm-diameter germanium light-flyers, respectively. The significant decrease can be attributed to much lower emissivity of germanium, which increases the temperature of germanium-coated samples compared to CNT-coated ones. Specifically, for the 2-cm-diameter disks under the optimal pressure (around 7 Pa) and 1.5 kW/m^2 incident irradiance, our model (discussed later) predicts a 450 K temperature for the germanium-coated samples at its optimal pressure, whereas that for the CNT-coated samples is 385 K. This discrepancy in the surface temperature suggests that a greater reduction in germanium's emissivity (up to 80% as discussed later) offsets the slight reduction in its TAC (only 10% difference as discussed later compared to CNT's 25%). Larger disks exhibited greater reductions in minimum irradiances due to their higher surface area and thus higher importance of radiative heat dissipation and lower relative importance of air conduction. Mathematical details of the emissivity's effect on the disk temperature and photophoretic force are described in the *Supplemental Material* [11].

Plotting the minimum irradiance needed for levitation versus the chamber pressure shows a parabola-like minimum in the log-log scale (Fig. 2). The photophoretic force was both predicted [13][14][15] and observed [12] to reach a maximum at pressures where the mean free path (MFP) is proportional to the disk diameter (i.e., for Kn ~ 0.047, where Kn is the Knudsen number, equal to the ratio of the gas's mean free path to the diameter of the levitating disk). The bottom of the parabola corresponds to the *optimal pressure* that maximizes the lift force.

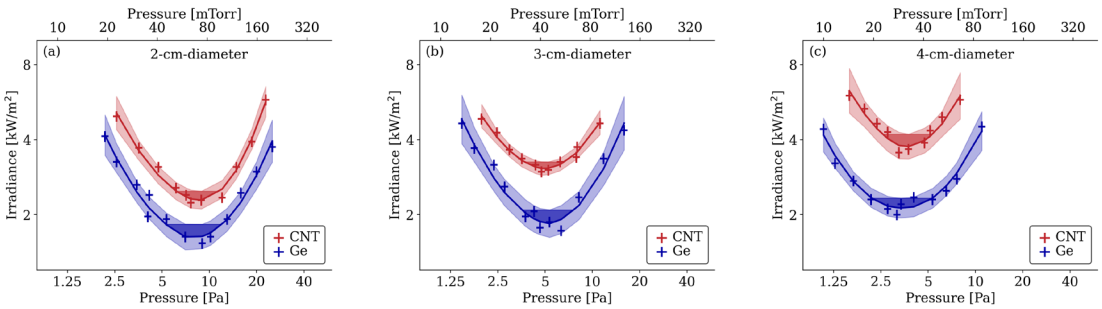

FIG. 2. Levitation performance of (a) 2, (b) 3, (c) 4-cm-diameter alumina-mylar disks with Ge or CNT absorber coatings. The flyers were launched from two aluminum rods (2.4 mm in diameter) that were placed far from the vacuum chamber's bottom (4.5 cm). Solid lines show locally estimated scatterplot smoothing (LOESS) fits, with 99% confidence intervals marked with light shading. Estimated optimal pressures and minimum irradiances are shown with darker shading.

We extensively characterized our films in order to better understand their optical and thermal accommodation properties. Our experiments included measuring the optical properties of our films using both thermal imaging and transmittance-only Fourier-transform infrared (FTIR) spectrometry to test our hypothesis that germanium leads to a lower emissivity than CNTs. We note that precise measurements of the material's optical properties requires rigorous analysis and a system consisting of the radiation source, sample, and detector. The ideal way to do this is to use a home-built FTIR spectrometer method with an emission measurement attachment [16] but rough estimates can be done *via* these thermal imaging and transmittance-only FTIR as detailed below. We also measured the films' TAC values using a concentric spherical-shell configuration [6] and their roughness using atomic force microscopy (AFM).

The ability of materials to lose heat by radiation is characterized by their emissivity (ε), which is related to their transmittance (t) and reflectance (r) at the same wavelength through the equation $\varepsilon = 1 - t - r$. First, we estimated the transmittance and reflectance at thermal infrared wavelengths using thermal imaging. To conduct this test, as shown in Fig. 3 (a, b), we used a hotplate as a radiation source and measured thermal infrared radiation transmitted and reflected by a light-flyer film at normal incidence using a thermal camera. The details are described in the *Supplemental Material* [11]. Subtracting 90-degree transmittance and reflectance from unity resulted in the emissivity of approximately 0.08 and 0.48 for germanium and CNT-based films, respectively, as tabulated in Table 1. Using a similar measurement in the optical frequency range, we also estimated the visible-range absorptivity of both CNT and germanium to be 0.75 using a white flashlight as the light source. It is highlighted that the optical data for mylar-alumna films are not listed in Table 1 because their optical properties vary little from bare mylar films and hence are of low interests.

TABLE 1. Optical properties and TAC for various materials.

Property	**Mylar**	**Mylar-Ge**	**Mylar-CNT**
IR transmittance	0.92±0.01	0.81±0.01	0.47±0.02
IR reflectance	0.02±0.01	0.11±0.01	0.05±0.01
IR emissivity	0.06±0.02	0.08±0.02	0.48±0.03
Visible transmittance	0.94±0.01	0.18±0.01	0.22±0.01

Visible reflectance	0.02±0.01	0.07±0.02	0.03±0.01
Visible absorptivity	0.03±0.02	0.75±0.03	0.75±0.02
TAC	0.77±0.03	0.90±0.03	1.08±0.05

As shown in Fig. 3(c), we also measured the transmittance of mylar, mylar-CNT, and mylar-germanium light-flyer materials at wavenumbers from 4000 to 400 cm^{-1} using a FTIR spectrometer. To estimate an upper bound for emissivity, we assumed zero reflectance of the films, giving the upper bound $\varepsilon_{max} = 1 - t$. Based on the expected temperatures of 400 to 500 K for a light-flyer under sunlight, spectral emission reaches a maximum at approximately 900 cm^{-1}, corresponding to 11 μm wavelength. Therefore, by averaging the transmittance in the range 900±400 cm^{-1}, where the blackbody radiation peaks at temperatures between 400-500 K, we derived the upper bound for emissivity to be 0.11 and 0.49 for germanium and CNT-based films, respectively, values that agree with those obtained through thermal imaging. Our results show that germanium has nearly five times lower emissivity than CNTs, resulting in significantly larger temperatures and a stronger photophoretic lift force.

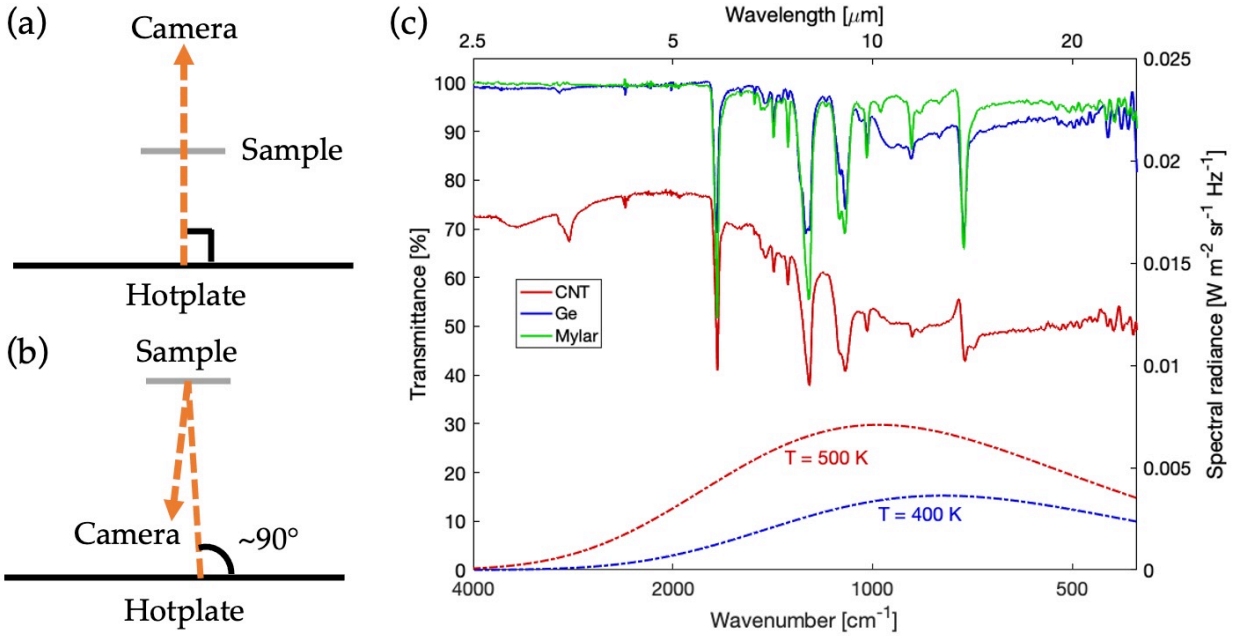

FIG. 3. Characterization results of optical properties from (a, b) thermal imaging and (c) transmittance-only FTIR. Schematics of the thermal imaging method measuring the 90-degree (a) transmittance and (b) reflectance. (c) The left axis plots the transmittance of various films as characterized by FTIR, while the right plots the calculated spectral radiance of black body radiation at 400 and 500 K surface temperature. The shaded area highlights the spectrum where transmittance is averaged.

Next, we characterized the TAC values of various surfaces using the experimental setup described in Ref. [6]. We first calibrated our experimental setup by comparing results of gold and platinum with literature values. We then prepared the same samples as for FTIR and averaged three sets of results for each of mylar, mylar-CNT, and mylar-germanium, and mylar-alumina, as tabulated in Table 1. Specifically, mylar-alumina had a TAC of 0.79±0.03. The measured TAC values between

0.8 and 1.1 in air are consistent with literature reports that the TAC is usually close to unity for interactions with relatively heavy molecules, such as nitrogen and oxygen [6][7][17]. We note that, although the TAC is defined to be between 0 and 1, the measured TAC may be slightly larger than unity due to the systematic measurement errors [18][19]. However, the differences between the TACs of any two materials, which is the quantity needed to predict photophoretic forces, are accurate even in the presence of such systematic errors. Our measurements, summarized in Table 1, show that the typical TAC difference between a top layer (e.g., mylar or alumina) and a bottom one (i.e., germanium or CNT) is approximately 0.1 for germanium-based light-flyers and 0.25 for CNT-based ones. Details are described in the *Supplemental Material* [11].

Surface roughness is one of the factors affecting TAC, with greater roughness typically resulting in a higher TAC because an incident molecule is more likely to collide multiple times with a rough surface and therefore reach a higher degree of thermalization. To better understand our TAC findings, we conducted Atomic Force Microscopy (AFM) of various surfaces we used for light-flyers. As shown in Fig. 4 (b-d), the root mean squared (RMS) roughness of mylar, mylar-germanium, and mylar-CNT were 2.5, 34.8, 71.2 nm, respectively. This upward trend aligns well with the TAC values presented in Table 1, where smoother surfaces have a lower RMS roughness and consequently lower TAC. Note that tall (100-400 nm) peaks observed in Fig. 4 (a, b) are associated with sub-micron particles intentionally included into the mylar sheet by the manufacturer to reduce stiction. These rare inclusions do not affect the number of collisions between a molecule and the surface and therefore were not included in the RMS roughness comparison. Environmental Scanning Electron Microscopy (e-SEM) images of these particles on both mylar and mylar-germanium surfaces are shown in Fig. S4.

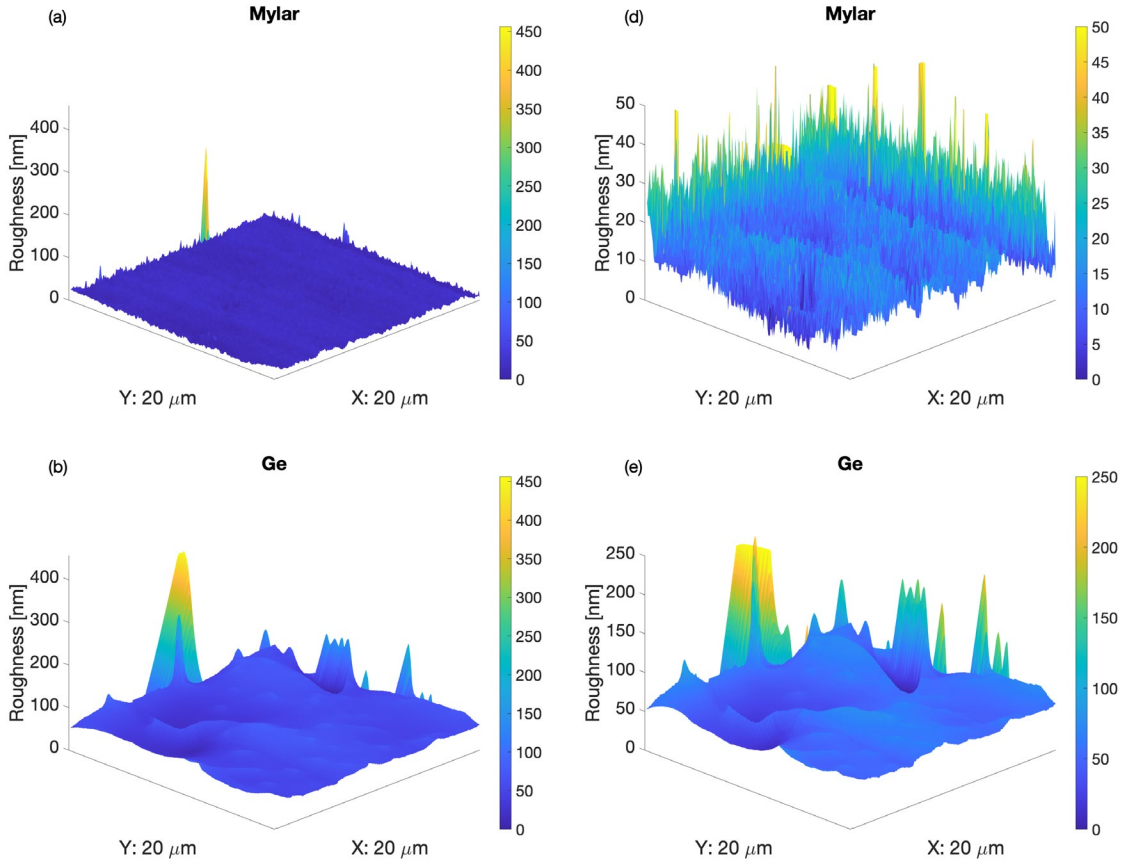

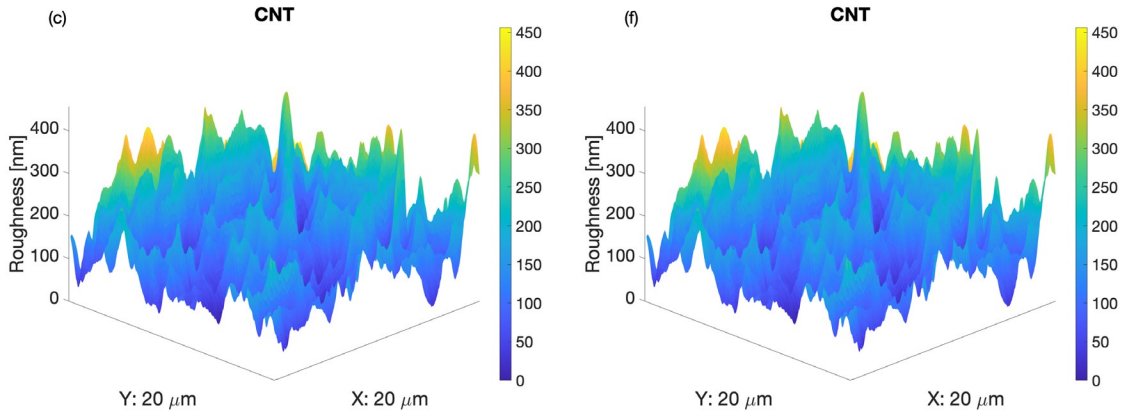

FIG. 4. Characterization results of surface properties from AFM. (a-c) are three-dimensional surface roughness graphs focusing on 20 μm by 20 μm spots for (a) mylar, (b) mylar-Ge, and (c) mylar-CNT surfaces. (d-f) are rescaled graphs to exclude friction enhancement particles.

Despite their lower TAC difference, the much lower emissivity of germanium-coated light-flyers still offers net advantages in real-world levitation applications in Earth's mesosphere or on Mars. It is therefore important to conduct experiments in a low-temperature vacuum chamber at the conditions of the mesosphere. While state-of-the-art techniques can cool down the vacuum chamber by approximately 100 K using dry ice or other vacuum cooling methods [20][21], these techniques are expensive and challenging to implement, especially under high optical flux. Instead, we performed experiments at room temperature and used them to develop a revised model for our light-flyers based on the photophoresis theory and our experimental data.

According to Rohatschek's work [14], the semi-empirical equation of the photophoretic force is $1/F = 1/(C_{fm}F_{fm}) + 1/(C_{cont}F_{cont})$, where F stands for the photophoretic force, subscripts fm and $cont$ for free-molecular and continuum regime, respectively, and C_{fm} and C_{cont} are typically assumed to be one for atmospheric aerosols [14][24]. In the free-molecular regime where the ambient pressure is low, the momentum difference in gas molecules colliding with the top and bottom surfaces exerts an upward force pointing from the high-TAC to low-TAC side. In the continuum regime where the ambient pressure is high, the thermal creep flow around the sample creates the reaction force in the same direction (pointing from the high-TAC to low-TAC side). For a sphere with no discontinuous boundaries, the main approximations used by Rohatschek were about the value of the thermal creep coefficient and the use of interpolation $1/F = 1/F_{fm} + 1/F_{cont}$. In our case, we take the limit of an oblate spheroid to approach the flat-disk light-flyer.

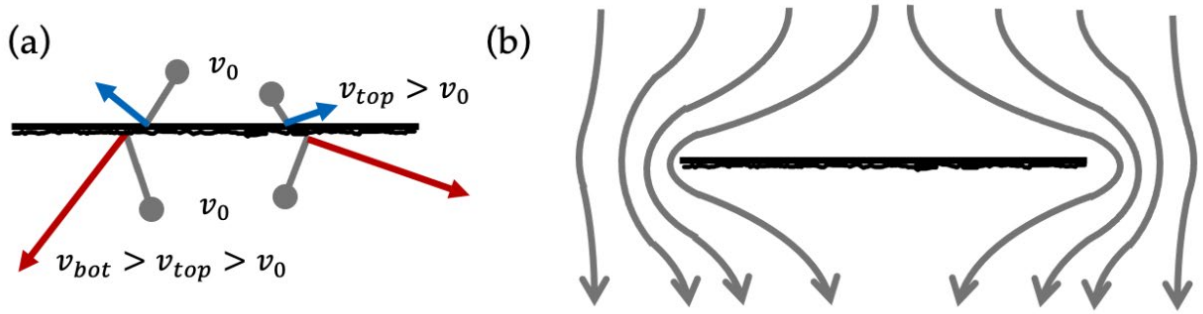

FIG. 5. Schematics of photophoretic forces in (a) free-molecular and (b) continuum regimes. v_0 denotes the initial velocities of gas molecules before colliding with the surface, while v_{top} and v_{bot} represent the velocities of gas molecules after colliding with the top and bottom surfaces, respectively.

However, the case of $C_{fm} = C_{cont} = 1$, valid for spherical microparticles, did not agree with our experimental observations of ultrathin disks. Instead, as shown in Fig. 5, $C_{fm} = 0.19$ and $C_{cont} = 2$ fitted our experimental observations at all pressures for all light-flyer sizes of both germanium and CNT-coated samples. Our use of C_{fm} and C_{cont} as fitting parameters is motivated by the recognition that the original semi-empirical interpolation method is most accurate in either free-molecular or continuum regimes and is least accurate in the transition regime. However, the $\Delta\alpha$-photophoretic force reaches its maximum in the transition regime where the physics involved is complex, which necessitates adjustments to these two coefficients. When dealing with significantly lower or higher pressures, $C_{fm} = C_{cont} = 1$ remains valid. Nevertheless, fitting is necessary in the transitional flow region before an accurate and comprehensive model can be developed specifically for the transition regime, which is most useful in practical applications. Specific equations for the derivation of light-flyer's temperature and photophoretic force are discussed in the *Supplemental Material* [11].

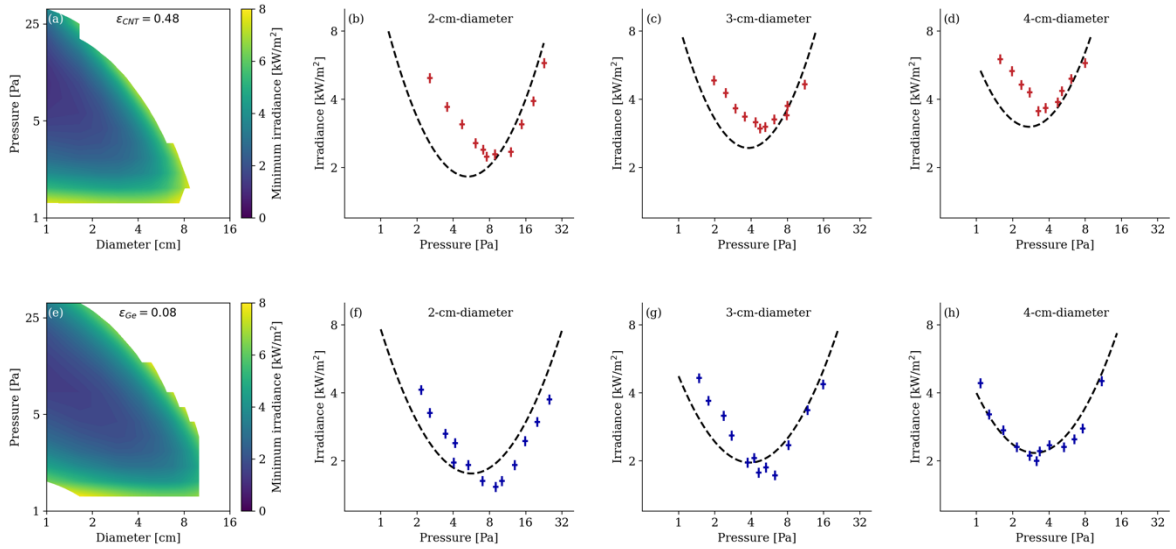

FIG. 6. Theoretical predictions and experimental data. Contour maps of the minimum irradiance for (a) CNT-coated disks (by assuming a uniform emissivity $\varepsilon_{CNT} = 0.48$) and (e) germanium-coated disks (by assuming $\varepsilon_{Ge} = 0.08$). Predicted irradiance-pressure curves and the experimental irradiance-pressure data for (b-d) CNT-coated disks and (f-h) germanium-coated disks with (b, f) 2, (c, g) 3, and (d, h) 4 cm diameters.

This theoretical model of the light-flyer's performance in our laboratory vacuum chamber can be applied to Earth's mesosphere as well. Earth's mesosphere extends from 50 to 100 km in altitude [22][23], with pressures ranging from 75 to 0.025 Pa (i.e., 560 to 0.19 mTorr). The ambient temperature in the mesosphere varies between 180 and 270 K, significantly lower than the room

temperature in our vacuum chamber (293 K). The high-altitude temperature profile therefore offers considerable room for performance improvements, such as more effective radiative heat dissipation and less thermal deformation of mylar.

Next, we considered the 2-cm-diameter germanium-coated light-flyer as an example since it had a lower minimum irradiance than the 3 and 4-cm-diameter disks. As shown in Fig. 6 (a), assuming a normal solar insolation of 1.36 kW/m^2 on top of Earth's atmosphere [25][26], this light-flyer could levitate between 67 and 75 km altitude, corresponding to a pressure range of 7.4 to 2.1 Pa (i.e., 56 to 16 mTorr). A more conservative estimate can be considered by assuming an incident angle of the sunlight smaller than 90 degrees, which would be typical for a light-flyers without any tilting mechanism [2]. Even at a 45-degree incident angle, the insolation would still be nearly 1.0 kW/m^2, narrowing the altitude range slightly to 69-73 km Fig. 6 (b) demonstrates the temperatures of the light-flyer at different solar irradiance levels: 1, 1.36, and 2 kW/m^2, corresponding to solar incident angles of 45 degrees, normal, and normal plus sunlight reflected due to ground albedo. Importantly, the temperatures remain significantly below the thermal deformation temperature of mylar, which is around 500 K. Hence, these results suggest that a long-lasting levitation in a 4-km-wide altitude range may be possible, despite strong wind shears in the mesosphere [26][27]. The outcomes for 3- and 4-cm-diameter disks are presented in Fig. S7 of *Supplemental Material* [11], indicating a gradual reduction in the operational pressure and altitude range.

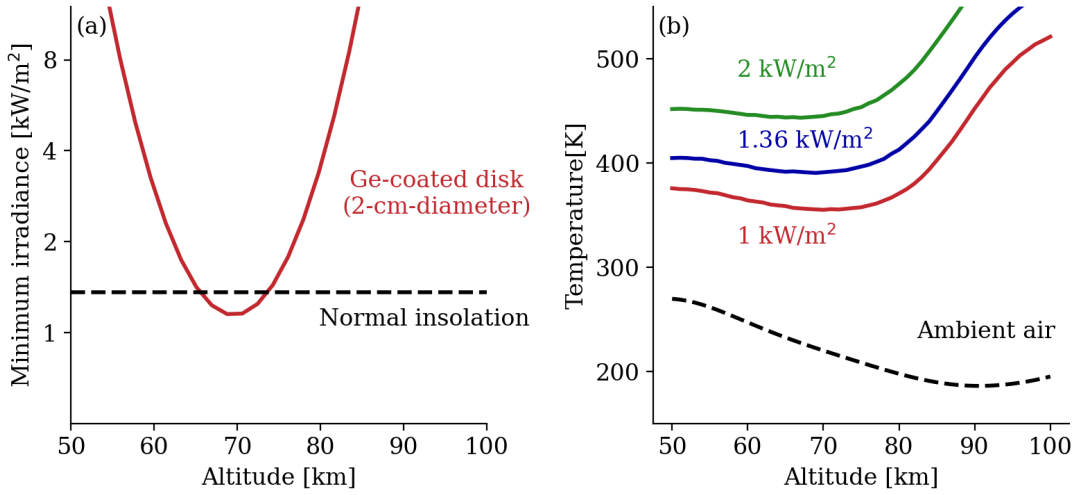

FIG. 7. Key predictions from the theoretical model. All plots assume a germanium-coated light-flyer with top TAC $\alpha_{top} = 0.9$, bottom TAC $\alpha_{bot} = 0.8$, uniform emissivity $\varepsilon = 0.08$, optical absorptivity $\epsilon_{vis} = 0.75$, and areal density $\rho = 1.0$ g/m^2. (a) The minimum irradiance required for a 2-cm-diameter light-flyer vs. altitude. The black dashed line stands for the normal solar insolation (i.e., 1.36 kW/m^2). (b) The temperature profiles of this 2-cm-diameter light-flyer at different irradiance levels and the ambient air versus altitude.

Maximum payloads can also be derived from the model, as discussed in the *Supplemental Material* [11]. For light-flyer disks a few centimeters in diameter, the payload is generally in the milligram range, which is challenging for practical applications. Similar (milligram range) payloads were predicted in Ref. [6] but those predictions assumed hypothetical values of emissivity and thermal

accommodation coefficient. Our predictions in the paper are fully based on experimentally measured properties. Moreover, Celenza et al. recently showed that 3D structures made from nanocardboard can increase the payload to the kilogram range [4]. Using germanium as a light-absorbing coating in these structures would greatly increase (approximately double) the photophoretic force by reducing the thermal emissivity.

Conclusion

In summary, we have demonstrated light-flyers composed of alumina and mylar as structural layers and germanium as a selective-absorber. Unlike most commonly used ceramic-metal selective absorbers [28], which are relatively thick, heavy, and have low emissivity because they are highly reflective in the thermal infrared, our ultrathin germanium layer are highly transparent in thermal infrared range. We conducted tests on germanium-coated disks with diameters of 2, 3, and 4 cm under minimized ground effect conditions and achieved successful levitations at irradiance levels as low as 1.5 kW/m^2 at room temperature. We characterized the optical and surface properties of germanium and CNT-based films and found germanium to have a sixfold lower emissivity. Using experimental data and semi-empirical photophoretic force, we developed a revised model and predicted levitation capabilities at various altitudes for light-flyers of multiple sizes. In addition to the two-dimensional photophoretic light-flyer disks, the germanium coating can be applied on three-dimensional geometries like Celenza's [4] balloon designs to reduce radiative heat loss and increase the photophoretic force, paving the way for future low-cost and clean-energy atmospheric research.

References

[1] J. Cortes, C. Stanczak, M. Azadi, M. Narula, S. M. Nicaise, H. Hu, and I. Bargatin, *Photophoretic Levitation of Macroscopic Nanocardboard Plates*, Advanced Materials **32**, (2020).

[2] B. C. Schafer, J. Kim, J. J. Vlassak, and D. W. Keith, *Analytical Models for the Design of Photophoretically Levitating Macroscopic Sensors in the Stratosphere*, ArXiv:2209.08093 (2022).

[3] M. Azadi, G. A. Popov, Z. Lu, A. G. Eskenazi, A. J. W. Bang, M. F. Campbell, H. Hu, and I. Bargatin, *Controlled Levitation of Nanostructured Thin Films for Sun-Powered near-Space Flight*, Sci Adv **7**, (2021).

[4] T. Celenza, A. Eskenazi, and I. Bargatin, *3D Photophoretic Aircraft Made from Ultralight Porous Materials Can Carry Kg-Scale Payloads in the Mesosphere*, ArXiv:2301.04281 (2023).

[5] C. D. F. Honig and W. A. Ducker, *Effect of Molecularly-Thin Films on Lubrication Forces and Accommodation Coefficients in Air*, The Journal of Physical Chemistry C **114**, 20114 (2010).

[6] H. Yamaguchi, T. Imai, T. Iwai, A. Kondo, Y. Matsuda, and T. Niimi, *Measurement of Thermal Accommodation Coefficients Using a Simplified System in a Concentric Sphere Shells Configuration*, Journal of Vacuum Science & Technology A: Vacuum, Surfaces, and Films **32**, (2014).

[7] D. J. Rader, J. N. Castaneda, J. R. Torczynski, T. W. Grasser, and W. M. Trott, *Measurements of Thermal Accommodation Coefficients (No. SAND2005-6084),* Sandia National Laboratories (SNL), Albuquerque, NM, and Livermore, CA, (2005).

[8] F. Zhuge, Z. Zheng, P. Luo, L. Lv, Y. Huang, H. Li, and T. Zhai, *Nanostructured Materials and Architectures for Advanced Infrared Photodetection*, Adv Mater Technol **2**, (2017).

[9] E. Takasuka, E. Tokizaki, K. Terashima, and S. Kimura, *Emissivity of Liquid Germanium in Visible and near Infrared Region*, J Appl Phys **82**, 2590 (1997).

[10] National Aeronautics and Space Administration, *SOFIA Offers New Way to Study Earth's Atmosphere*, https://www.nasa.gov/missions/station/sofia-offers-new-way-to-study-earths-atmosphere/ (2021).

[11] See Supplemental Material at "link" for the details on the vacuum chamber and light emitting diode (LED) setup; launchpad selection; levitation performance of another set of light-flyers; light-flyer fabrication procedure and characterization; TAC measurement and data processing; theoretical modeling for light-flyers; and prediction of light flyers for mesospheric applications. The Supplemental Material also contains Refs. [29–31].

[12] Z. Lu, M. Stern, J. Li, D. Candia, L. Yao-Bate, T. J. Celenza, M. Azadi, M. F. Campbell, and I. Bargatin, *Minimizing the Ground Effect for Photophoretically Levitating Disks*, Phys Rev Appl **19**, 044004 (2023).

[13]. Rohatschek, *Photophoresis and Accommodation.*, Оптика Атмосферы и Океана **21**, 87 (2014).

[14] H. Rohatschek, *Semi-Empirical Model of Photophoretic Forces for the Entire Range of Pressures*, J Aerosol Sci **26**, 717 (1995).

[15] N. T. Tong, *Photophoretic Force in the Free Molecule and Transition Regimes*, J Colloid Interface Sci **43**, 78 (1973).

[16] K. Mizuno, J. Ishii, H. Kishida, Y. Hayamizu, S. Yasuda, D. N. Futaba, M. Yumura, and K. Hata, *A Black Body Absorber from Vertically Aligned Single-Walled Carbon Nanotubes*, Proceedings of the National Academy of Sciences **106**, 6044 (2009).

[17] W. M. Trott, J. N. Castañeda, J. R. Torczynski, M. A. Gallis, and D. J. Rader, *An Experimental Assembly for Precise Measurement of Thermal Accommodation Coefficients*, Review of Scientific Instruments **82**, (2011).

[18]W. Trott, D. Rader, J. Castaneda, J. Torczynski, and M. Gallis, *Experimental Measurements of Thermal Accommodation Coefficients for Microscale Gas-Phase Heat Transfer,* 39th AIAA Thermophysics Conference 4039 (2007).
[19]P. T. C. Chen, R. J. Hedgeland, and S. R. Thomson, *Surface Accommodation of Molecular Contaminants*, Optical System Contamination: Effects, Measurement, Control II, 1329 (1990).
[20]W. Burgmann and K. Göhler, *Modern Vacuum Pumps for the Vacuum Degassing of Steel in Small and Large Vacuum-Degassing Units*, Metallurgist **57**, 516 (2013).
[21]S. Thiangchanta, T. A. Do, W. Tachajapong, and Y. Mona, *Experimental Investigation of the Thermoelectric Cooling with Vacuum Wall System*, Energy Reports **6**, 1244 (2020).
[22]H. Rohatschek, *Direction, Magnitude and Causes of Photophoretic Forces*, J Aerosol Sci **16**, 29 (1985).
[23]M. Venkat Ratnam, A. K. Patra, and B. V. Krishna Murthy, *Tropical Mesopause: Is It Always Close to 100 km?*, Journal of Geophysical Research: Atmospheres **115**, (2010).
[24]U. von Zahn, J. Höffner, V. Eska, and M. Alpers, *The Mesopause Altitude: Only Two Distinctive Levels Worldwide?*, Geophys Res Lett **23**, 3231 (1996).
[25]O. Coddington, J. L. Lean, P. Pilewskie, M. Snow, and D. Lindholm, *A Solar Irradiance Climate Data Record*, Bull Am Meteorol Soc **97**, 1265 (2016).
[26]L. Qian, C. Jacobi, and J. McInerney, *Trends and Solar Irradiance Effects in the Mesosphere*, J Geophys Res Space Phys **124**, 1343 (2019).
[27]A. Müllemann and F.-J. Lübken, *Horizontal Winds in the Mesosphere at High Latitudes*, Advances in Space Research **35**, 1890 (2005).
[28]C. E. Kennedy, *Review of Mid-to High-Temperature Solar Selective Absorber Materials (No. NREL/TP-520-31267)*, National Renewable Energy Lab., (2002).
[29]W. M. Trott, D. J. Rader, J. N. Castañeda, J. R. Torczynski, M. A. Gallis, and T. Abe, *Measurement of Gas-Surface Accommodation*, *AIP Conference Proceedings*, 621, (2008).
[30]*U.S. Standard Atmosphere vs. Altitude,* https://www.engineeringtoolbox.com/standard-atmosphere-d_604.html (n.d.).
[31]R. Carmichael, *A Table of the Standard Atmosphere to 86 Km in SI Units,* https://www.pdas.com/atmosTable1SI.html (2021).